

000
001
002
003
004
005
006
007
008
009
010
011
012
013
014
015
016
017
018
019
020
021
022
023
024
025
026
027
028
029
030
031
032
033
034
035
036
037
038
039
040
041
042
043
044
045
046

KVCACHE-CENTRIC MEMORY FOR LLM AGENTS

Anonymous authors
Paper under double-blind review

ABSTRACT

LLM agents in complex, long-horizon workflows are constrained by the model’s context window. Current plaintext-based memory systems suffer from unstable retrieval accuracy and disrupt prefix caching, harming both performance and efficiency. We propose MemArt, a novel memory paradigm that operates directly within the LLM-native format: the key-value (KV) cache. Instead of using plaintext, MemArt stores conversational turns as reusable KV cache blocks and retrieves relevant memories by computing attention scores in latent space. To enable accurate and efficient retrieval, we develop a multi-token aggregation retrieval strategy that uses compressed keys for efficient KV selection and a decoupled position encoding mechanism to ensure retrieved blocks are safely and coherently reused. On the LoCoMo benchmark, MemArt improves accuracy by over 11% (up to 39.4%) compared to state-of-the-art plaintext-based memory methods, nearly matching full-context performance. Critically, it achieves this while reducing prefill tokens by over two orders of magnitude (91-135 \times), representing a significant leap forward for building powerful and efficient long-context agents.

1 INTRODUCTION

“The true art of memory is the art of attention.” — Samuel Johnson, English writer

Large language model (LLM) agents are emerging as a new paradigm for applying foundation models in complex, real-world workflows, including scientific exploration (e.g., deep research (Xu & Peng, 2025)), coding assistants (Liu et al., 2024), and autonomous task planning systems (Wang et al., 2024a). Unlike single-turn prompting or short-lived chatbots, these agents are designed to operate over extended horizons, often spanning hours or days of execution and involving tens to hundreds of iterative LLM calls. During such long-running sessions, agents continuously accumulate rich context that quickly grows beyond the context window of even frontier models with million-token capacities (Google DeepMind, 2025). To address this scalability bottleneck, recent work has introduced external memory systems that store and selectively retrieve historical context (Chhikara et al., 2025; Rasmussen et al., 2025; Amazon Web Services, 2025). Such memory mechanisms are essential for sustaining reasoning efficiency, accuracy, and robustness in long-horizon agent workflows.

Most deployed memory systems, including Mem0 (Chhikara et al., 2025), Zep (Rasmussen et al., 2025), and AWS AgentCore memory (Amazon Web Services, 2025), adopt plaintext-based memory. They segment or summarize historical context into sentence-level memory entries, which are then indexed and retrieved using vector databases or graph structures. While straightforward, this approach exhibits two fundamental limitations. First, context summarization and retrieval based on vector similarity or graph traversal often fail to preserve the full semantic dependencies of long, multi-turn interactions. As a result, the retrieved memory may omit critical context or include irrelevant information, leading to degraded LLM inference performance compared to full-context inference. Second, the segmentation and summarization of historical context into discrete memory entries disrupts the natural sequential structure of prompt prefixes. Modern LLM engines

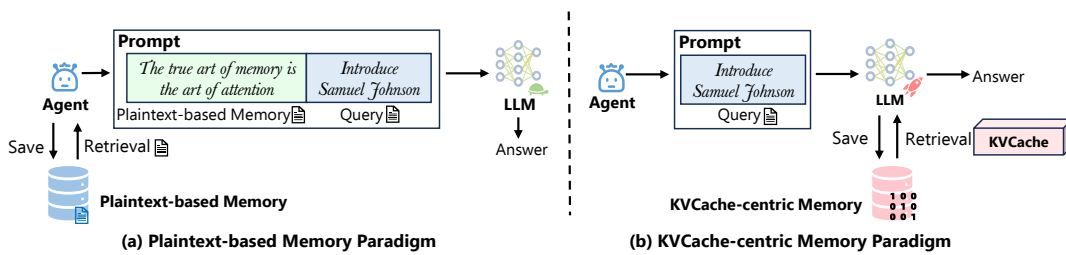


Figure 1: Paradigm comparison between plaintext-based memory and KVCache-centric memory. In the plaintext paradigm (a), the agent must explicitly retrieve and insert memory into the prompt, which often leads to inaccurate retrieval and breaks prefix caching. In the KVCache-centric paradigm (b), the LLM natively stores and reuses KV blocks, so the agent only issues the new query, enabling more accurate retrieval in latent space and efficient prefill reuse.

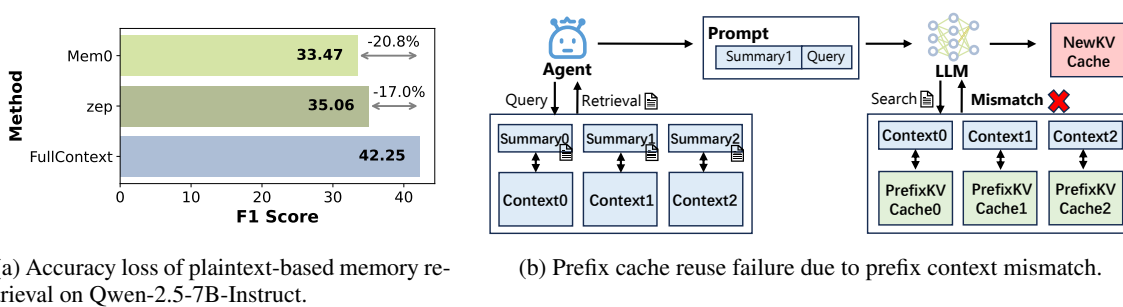
accelerate inference using prefix caching (Qin et al., 2025; Gao et al., 2024; Zheng et al., 2024)—reusing the key-value (KV) cache of shared prefixes across calls—but segmented and summarized memory introduces prefix discontinuities, undermining these efficiency gains.

We propose MemArt, a new memory paradigm that shifts from plaintext-based memory to *KVCache-centric memory* to enhance both performance and efficiency. As illustrated in Figure 1, instead of managing plaintext, MemArt stores historical context directly as reusable KV blocks and retrieves relevant memory by computing attention scores between the current prompt and the stored KV blocks in latent space. This approach offers three key advantages: (1) *High-Fidelity Retrieval*: Operating in latent space allows retrieval to align directly with the model’s attention mechanism, offering superior semantic accuracy compared to methods relying on plaintext similarity. (2) *Maximal Inference Efficiency*: Retrieved KV blocks are directly reused during prefill, eliminating redundant token processing and significantly reducing computational overhead and latency. (3) *Seamless Integration*: The entire framework is model-agnostic and functions as a plug-and-play component, requiring no modifications to model weights or architecture.

Despite its promise, achieving KVCache-centric memory introduces two key challenges. First, *how can we perform high-fidelity retrieval without a full memory scan?* As the memory grows, exhaustively scanning every KV block to find the most relevant ones becomes computationally prohibitive. The challenge lies in designing a mechanism that can quickly identify the most salient memories from a large repository without sacrificing accuracy. Second, *how to ensure the safe reuse of retrieved KV blocks?* A standard KV cache that can reuse corresponds to a single, contiguous prefix. Retrieved blocks, however, are non-contiguous and carry their original positional information. Simply concatenating them creates a positionally incoherent sequence that disrupts the model’s attention, ultimately harming output quality.

For efficient and accurate retrieval, MemArt first computes a compressed representative key for each KV block to enable a fast search that avoids a full memory scan. It then employs a multi-token aggregation retrieval strategy that synthesizes attention scores from all prompt tokens to ensure the final selection is highly relevant. For safe reuse, MemArt uses a decoupled position encoding mechanism. This component validates and adjusts the positional information of retrieved blocks, guaranteeing they can be integrated into the current context without creating positional conflicts.

We evaluate MemArt on the widely used LoCoMo benchmark (Maharana et al., 2024). Experimental results show that MemArt improves inference accuracy by 11.8–39.4% over state-of-the-art plaintext-based memory approaches, approaching the performance of full-context inference. Critically, it reduces 91–135× prefill tokens over plaintext-based memory approaches. These results highlight KVCache-centric memory as a promising foundation for accurate and efficient long-context LLM agents.



(a) Accuracy loss of plaintext-based memory retrieval on Qwen-2.5-7B-Instruct.
 (b) Prefix cache reuse failure due to prefix context mismatch.

Figure 2: Limitations of plaintext-based memory: accuracy degradation and prefix cache reuse failure.

2 BACKGROUND AND RELATED WORK

Prefix Caching in LLM Inference LLMs based on the Transformer architecture generate tokens autoregressively, with each token attending to all preceding tokens. To avoid redundant computation, the key (K) and value (V) tensors of previous tokens are stored as KVCache, enabling the prefill phase to cache K and V for the input prompt and the decode phase to generate new tokens by computing K and V only for the latest token. Building on this mechanism, prefix caching accelerates inference by sharing the KVCache of identical prefixes across requests, and has been widely adopted in recent systems to reduce computation and latency (Kwon et al., 2023; Zheng et al., 2024; Qin et al., 2025; Yao et al., 2025; Gao et al., 2024).

Plaintext-Based Memory for LLM Agents Plaintext-based methods explicitly store and manipulate information in human-readable form. Early systems such as MemoryBank (Zhong et al., 2024) and MemGPT (Packer et al., 2023) rely on predefined policies for storage, integration, and retrieval. Recent efforts shift toward structured representations, such as temporal knowledge graphs in Zep (Rasmussen et al., 2025), atomic notes in A-MEM (Xu et al., 2025), and hierarchical graph memories in Mem0 (Chhikara et al., 2025), which capture relational, temporal, and hierarchical dependencies but remain rule-based. Recent efforts also conceptualize memory as an operating system. MemoryOS (Kang et al., 2025) defines dynamic updates from short- to mid- to long-term memories, while MemOS (Li et al., 2025) defines unified representation, scheduling, and evolution across different memory types. However, MemOS does not provide detailed mechanisms for how these memory types coordinate or transform among each other. In parallel, Memory-R1 (Yan et al., 2025) employs a reinforcement learning based manager to learn memory operations, though at the cost of significant training overhead.

Limitations of Plaintext-Based Memory Plaintext-based memory suffers from two inherent limitations:

1) Accuracy Degradation: As shown in Figure 2(a), we evaluate the plaintext-based memory retrieval baseline Mem0 (Chhikara et al., 2025) and Zep (Rasmussen et al., 2025) on the LoCoMo benchmark with the Qwen-2.5-7B-Instruct model, which exhibit F1 gaps of 20.8% and 17.0%, respectively, compared to full-context inference. This highlights the difficulty of plaintext-based summarization and similarity retrieval in capturing long-range semantic dependencies. Critical information is frequently omitted, while irrelevant segments are introduced, both of which harm downstream reasoning.

2) Prefix Caching Invalidation: Prefix caching reuses the KV cache only when exact prompt prefixes match. However, plaintext memory systems typically segment, summarize, or alter historical context, breaking textual continuity. As illustrated in Figure 2(b), this textual mismatch prevents cache reuse and forces costly recomputation of the KV cache, undermining one of the most important efficiency gains in modern LLM inference.

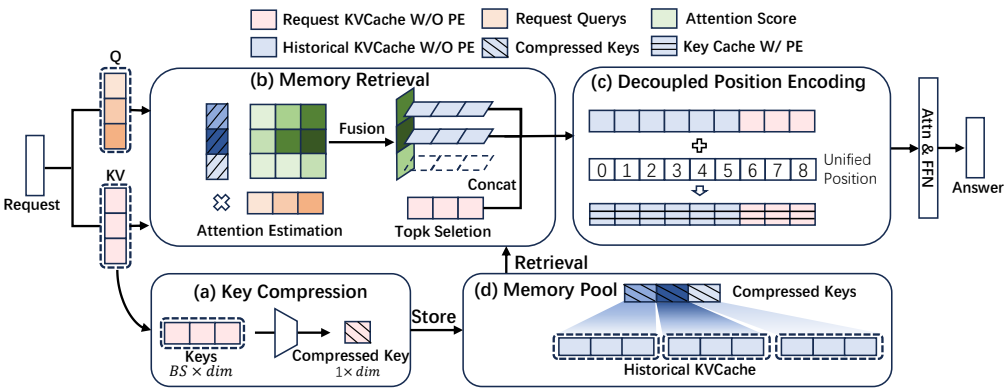


Figure 3: The architectural overview of MemArt.

3 MEMART: KVCACHE-CENTRIC AGENT MEMORY

To improve both performance and efficiency of agent inference, we propose MemArt, a new paradigm we term *KVCache-centric memory*. Instead of using plaintext, MemArt stores the KV cache as LLM-native memory. For each new request, MemArt identifies the most relevant historical KV blocks via latent-space attention and seamlessly reuses them for prefill. This design inherently yields three advantages: superior retrieval accuracy, dramatic gains in inference efficiency, and seamless plug-and-play integration. We now detail the MemArt framework and its core algorithmic components.

3.1 OVERALL FRAMEWORK

To enable efficient storage, retrieval, and reuse of KVCache-centric memory, MemArt adopts the framework shown in Figure 3, which comprises four key components:

- Key Compression:** Historical memory is stored as fixed-size KV blocks, each assigned a compressed key derived from its key set, providing a lightweight index that reduces retrieval overhead.
- Memory Retrieval:** For a new query request, attention scores are computed between the Q heads of all query tokens and compressed keys. The top- k most relevant KV blocks are selected via multi-token aggregation retrieval and reused in the prefill phase.
- Decoupled Position Encoding:** Since historical memory may exceed the context window of LLMs, positional misalignment can weaken attention and degrade inference. To address this, KV blocks are stored without positional encodings and later re-embedded with new encodings after retrieval, ensuring alignment within the current context window and consistency for downstream attention.
- Memory Pool:** A centralized memory pool manages the collection of KV blocks, each indexed by its compressed key for efficient organization and access.

Building on these components, the inference workflow follows Algorithm 1: (i) retrieve query-relevant memory using compressed keys, (ii) concatenate the retrieved KV blocks with the KV cache of the query request, (iii) re-embed new positional encodings to align within the context window, and (iv) compute memory-augmented attention. Meanwhile, the memory pool is asynchronously updated with newly generated KV cache and its compressed keys. Formally, the process is given by:

$$O = \text{Attn}(\text{EmbPE}(Q, \text{Concat}(K_M, K)), \text{Concat}(V_M, V)) \quad (1)$$

where K_M, V_M denotes the KV blocks retrieved from MemArt.

188 **Algorithm 1** Inference Workflow with MemArt

```

190 1: Input: Current Query  $Q$ , Current KVCache ( $K_{curr}, V_{curr}$ )
191 2: Memory: Compressed Indices  $CompK$ , Memory Pool ( $K_{mem}, V_{mem}$ )
192   # Memory Augmented Generation
193 3:  $(K_M, V_M) \leftarrow \text{Retrieve}(Q, CompK)$  # Query-Aware Memory Retrieval
194 4:  $K_{aug} \leftarrow \text{Concat}(K_M, K_{curr}), V_{aug} \leftarrow \text{Concat}(V_M, V_{curr})$  # Memory Integration
195 5:  $Q', K'_{aug} \leftarrow \text{EmbPE}(Q, K_{aug})$  # Align positional encodings
196 6:  $O \leftarrow \text{Attention}(Q', K'_{aug}, V_{aug})$  # Augmented Attention Computation
197   # Memory Pool Update (Asynchronous)
198 7:  $K_{mem} \leftarrow \text{Append}(K_{mem}, K_{curr}), V_{mem} \leftarrow \text{Append}(V_{mem}, V_{curr})$ 
199 8:  $CompK \leftarrow \text{Append}(CompK, \text{Compress}(K_{curr}))$  # Key Compression
200 9: Return: Output  $O$ 

```

201 3.2 ALGORITHM DESIGN

202 This subsection details the design of the core components of MemArt, including the key compression algorithm, the memory retrieval strategy, and the decoupled positional encoding.

203 3.2.1 AABB-BASED KEY COMPRESSION

204 The generated KV cache is partitioned into memory blocks of size BS and stored in a memory pool. To enable efficient retrieval, each key block K is compressed into an axis-aligned bounding box (AABB) (Van den 205 Bergen, 1997; Cai et al., 2014; Chen et al., 2024), defined by the maximum and minimum vectors that 206 enclose all key vectors within the block, as shown in Equation 2. This compact representation preserves 207 coarse-grained semantic information while avoiding exhaustive comparisons with individual key vectors, 208 thereby enabling rapid and accurate retrieval.

$$\begin{aligned}
 s^{\min}(K) &= (\min_{i=1}^{BS} k_{i,1}, \min_{i=1}^{BS} k_{i,2}, \dots, \min_{i=1}^{BS} k_{i,dim}) \in \mathbb{R}^{1 \times dim} \\
 s^{\max}(K) &= (\max_{i=1}^{BS} k_{i,1}, \max_{i=1}^{BS} k_{i,2}, \dots, \max_{i=1}^{BS} k_{i,dim}) \in \mathbb{R}^{1 \times dim}
 \end{aligned} \tag{2}$$

209 AABB compression is well-suited for high-dimensional keys because it is lightweight ($2 \times dim$ values per 210 block), preserves coordinate-wise extrema without distortions from projections like principal component 211 analysis (PCA) (Hotelling, 1933), and provides a natural coarse-grained filter before fine-grained attention.

212 3.2.2 MULTI-TOKEN AGGREGATION BASED MEMORY RETRIEVAL

213 Our retrieval process operates at the block level, building on the principle that neighboring keys in a KV 214 cache often share semantic importance (Jiang et al., 2024). To do this efficiently, we retrieve memory at 215 the block level using the compressed keys introduced earlier. Following Arkvale (Chen et al., 2024), the 216 relevance between a single query token $q \in \mathbb{R}^{1 \times dim}$ and block $K \in \mathbb{R}^{BS \times dim}$ is defined as the maximum 217 dot product:

$$I(q, K) = \sum_{i=1}^{dim} \max(q_i s_i^{\max}(K), q_i s_i^{\min}(K)) \tag{3}$$

218 This formulation provides an upper-bound estimate of the attention scores between q and all keys within 219 K , without exhaustively comparing each key. Consequently, $I(q, K_1) > I(q, K_2)$ indicates that block K_1 220 contains at least one key vector whose attention with q exceeds that of every key in K_2 .

235 Table 1: Formulations of normalization and aggregation strategies for multiple token relevance scoring.
236

237 Normalization	238 Aggregation	239 Formula for $I(Q, K)$	240 Notes
241 Softmax	242 Sum	$\sum_{q \in Q} \frac{\exp(I(q, K))}{\sum_{K' \in \mathcal{K}} \exp(I(q, K'))}$	243 Sharp normalization; 244 Balances all tokens.
245 Softmax	246 Max	$\max_{q \in Q} \frac{\exp(I(q, K))}{\sum_{K' \in \mathcal{K}} \exp(I(q, K'))}$	247 Sharp normalization; 248 Selects the strongest token.
249 Reciprocal Rank	250 Sum	$\sum_{q \in Q} \frac{1}{\text{rank}_q(K) + c}$	251 Smooth normalization; 252 Balances all tokens.
253 Reciprocal Rank	254 Max	$\max_{q \in Q} \frac{1}{\text{rank}_q(K) + c}$	255 Smooth normalization; 256 Selects the strongest token.

250 Nevertheless, unlike the decoding scenario that Arkvale targets (Chen et al., 2024), which uses a single
251 query token, agent memory retrieval occurs during prefill and must account for a multi-token prompt Q .
252 This introduces a key challenge: relevance scores from different query tokens are not directly comparable,
253 and different tokens may prioritize different memory blocks. A naive aggregation (e.g., averaging) would
254 dilute these varied signals.

255 To create a unified relevance score for the entire prompt, we introduce a two-step aggregation procedure:

$$256 I(Q, \mathcal{K}) = \text{Agg}_{q \in Q} (\text{Norm}_{K \in \mathcal{K}} (I(q, K))) \quad (4)$$

257 Here, \mathcal{K} denotes the collection of all compressed keys. The process works as follows: (1) *Normalize per*
258 *Token*: For each query token $q \in Q$, we first normalize its relevance scores $\{I(q, K) \mid K \in \mathcal{K}\}$ across
259 all compressed keys. This crucial step makes the scores from different tokens comparable. (2) *Aggregate*
260 *across Tokens*: Next, we aggregate these normalized scores across all query tokens to produce a single, final
261 relevance score for each block.

262 We systematically consider several strategies for these two steps (Table 1). For Normalization, we can use
263 *Softmax* to amplify the strongest signals or *Reciprocal-Rank* to create a smoother distribution that is less
264 sensitive to outliers (Cormack et al., 2009). For Aggregation, we can employ *Sum* to weigh evidence from
265 all tokens and *Max* to prioritize the single strongest token-block interaction.

266 Finally, based on the aggregated scores $I(Q, \mathcal{K})$, we select the top- k memory blocks. For efficiency, the
267 same set of k blocks is selected for all attention heads. These blocks are then concatenated in their original
268 chronological order to preserve temporal consistency for the final prefill computation.

269 3.2.3 DECOUPLED POSITIONAL ENCODING

270 A major challenge in reusing KV cache as long-term memory is the misalignment of positional embed-
271 dings across temporal spans. Cached key-value states with their original positional encodings can cause (i)
272 incoherent attention when historical tokens’ positions no longer match their locations in the reconstructed
273 sequence, and (ii) positions exceeding the model’s context window, leading to inference failure.

274 We address this by decoupling positional information from the stored KV cache. During storage, we omit
275 the rotary positional encoding (RoPE) (Su et al., 2024) and preserve only content-dependent KV cache:

$$276 K_i^{\text{raw}} = W_k x_i, \quad V_i^{\text{raw}} = W_v x_i, \quad (5)$$

277 where x_i is the hidden state of the i -th token, and W_k, W_v are the key and value projection matrices. At
278 inference, after retrieving top- k memory blocks $\{K_{i_1}^{\text{raw}}, \dots, K_{i_K}^{\text{raw}}\}$ based on the current query Q , the memory

282 tokens are concatenated in historical order and re-encoded with a unified positional scheme:
 283

$$284 \quad \tilde{Q}_j = R_{p(j)} Q_j^{\text{raw}}, \quad \tilde{K}_j = R_{p(j)} K_j^{\text{raw}}, \quad \tilde{V}_j = V_j^{\text{raw}}, \quad (6)$$

285 where $p(\cdot)$ is the absolute position in the concatenated sequence and the RoPE rotation matrix R_p . This
 286 ensures queries and historical memory share consistent positional information.
 287

288 For example, if a query Q contains three tokens and one memory block $\{K_{16}, K_{17}, \dots, K_{23}\}$ is selected,
 289 after concatenation, the K s in the memory block are reassigned positions $p(K) = [0, 1, \dots, 7]$ and the query
 290 tokens have $p(Q) = [8, 9, 10]$. Applying RoPE re-encodes all tokens into a unified positional space, enabling
 291 coherent attention across memory and query.
 292

293 4 EVALUATION

294 4.1 EXPERIMENTAL SETUP

295 **Datasets and Models** We adopt the LoCoMo benchmark (Maharana et al., 2024), a widely used suite for
 296 assessing long-term conversational memory in agent systems. It comprises 10 conversations, each contain-
 297 ing an average of 589 dialogues and 13,960 words. To enable precise evaluation, each dialogue is paired
 298 with approximately 200 questions and their corresponding correct answers, allowing models to be tested on
 299 retrieving specific details from the full conversation history. We exclude the adversarial subset, as it does not
 300 provide ground-truth answers. We implement MemArt on top of HuggingFace Transformers (Wolf et al.,
 301 2020), and all experiments are conducted on LLaMA-3.1-8B-Instruct (Grattafiori et al., 2024), Qwen-2.5-
 302 7B-Instruct (Yang et al., 2025b) and [Qwen-3-32B-A3B-Instruct \(Yang et al., 2025a\)](#).
 303

304 **Metrics** Following prior work (Chhikara et al., 2025; Li et al., 2025), we evaluate inference accuracy using
 305 two categories of metrics: lexical similarity and semantic correctness. Lexical similarity is measured with
 306 F1 Score (F1) and BLEU-1 (B1), which capture token-level overlap. Semantic correctness is measured with
 307 BERTScore-F1 (BERT) and cosine similarity (Sim) over sentence embeddings, reflecting meaning-level
 308 alignment. The average of these four metrics provides a more holistic measure of generation quality.
 309

310 **Baselines** We compare MemArt against following representative baselines: (1) **Full-Context Inference**:
 311 The entire dialogue history is provided as input to the LLMs. (2) **Zep**: A retrieval-oriented agent that
 312 implements structured memory access strategies, enabling effective reasoning over temporally extended and
 313 multi-turn queries (Rasmussen et al., 2025). (3) **Mem0**: A modular memory architecture featuring explicit
 314 in-context memory operations, designed to facilitate scalable deployment while maintaining high retrieval
 315 fidelity (Chhikara et al., 2025). (4) **H2O**: A KV cache sparse approach that retains heavy-hitter keys to
 316 shrink the active KV set during current inference (Zhang et al., 2023).
 317

318 4.2 MAIN RESULTS

319 We evaluate MemArt on the LoCoMo benchmark against Mem0 and Zep using LLaMA-3.1-8B-Instruct
 320 (L3), Qwen-2.5-7B-Instruct (Q2), and Qwen-3-32B-A3B-Instruct (Q3). To ensure fairness, we tune each
 321 method so that their KV lengths during decoding are comparable. MemArt uses a block size of 16 with
 322 top- k =128 (Softmax-Max) for L3 and Q3, and top- k =256 (RR-Max) for Q2. Mem0 is set to top- k =100 for
 323 L3/Q3 and 150 for Q2, while Zep uses top- k =20 for L3/Q3 and 25 for Q2. For the KV cache sparse method
 324 H2O, we configure it to use the same heavy KV cache budget as MemArt.
 325

326 4.2.1 PERFORMANCE COMPARISON

327 Table 2 shows the performance comparison of MemArt and the baselines on LoCoMo.
 328

329
 330 Table 2: Performance comparison between MemArt and baselines on the LoCoMo benchmark. Models are
 331 assessed on F1, B1, BERT, and Sim metrics (higher is better). Aver.S denotes the average across metrics.
 332 Best scores are in bold; second-best are underlined.

Method	LLaMA-3.1-8B-Instruct					Qwen-2.5-7B-Instruct					Qwen-3-30B-A3B-Instruct				
	F1	B1	BERT	Sim	Aver.S	F1	B1	BERT	Sim	Aver.S	F1	B1	BERT	Sim	Aver.S
FullContext	48.12	40.34	64.24	74.10	56.70	42.45	35.79	61.52	70.97	52.68	<u>51.06</u>	43.65	66.29	76.21	59.30
Zep	30.60	24.67	45.76	64.98	41.50	35.06	28.14	56.60	66.72	46.63	<u>42.23</u>	36.17	61.19	72.15	53.18
Mem0	26.86	21.60	53.18	60.93	40.64	33.47	28.36	57.68	66.55	46.51	<u>34.96</u>	28.85	58.16	68.10	47.51
H2O	38.48	30.90	59.38	68.42	49.29	29.44	22.32	54.03	62.51	42.07	40.77	32.43	59.86	69.16	50.55
MemArt	47.72	40.29	64.25	74.43	56.67	41.67	33.54	61.92	71.35	52.12	51.54	44.54	67.86	76.39	60.08

333
 334 Table 3: Efficiency comparison between MemArt and baselines on the LoCoMo benchmark.

Method	LLaMA-3.1-8B-Instruct		Qwen-2.5-7B-Instruct		Qwen-3-30B-A3B-Instruct	
	# Prefill Tokens	KV Length (Decode)	# Prefill Tokens	KV Length (Decode)	# Prefill Tokens	KV Length (Decode)
FullContext	21,892	21,912	22,125	22,145	22,125	22,145
Zep	3,285	3,305	4,160	4,180	3,491	3,511
Mem0	2,911	2,931	4,982	5,002	2,879	2,899
H2O	21,892	2,304	22,125	4,352	22,125	2,304
MemArt	32	2,100	37	4,153	37	2,105

349 MemArt reaches 99.9% of FullContext accuracy on L3, 98.9% on Q2, and 101.3% on Q3, showing that it
 350 nearly matches full-context generation while retrieving only a small fraction of memory. **Relative to Zep**
 351 and **Mem0**, MemArt improves accuracy by 36.5%/39.4% on L3, 11.8%/12.1% on Q2, and 12.9%/26.4% on
 352 Q3, respectively. **Compare to KV Cache pruning method H2O**, MemArt improves accuracy by 14.9% on
 353 L3, 23.9% on Q2, and 18.8% on Q3, respectively.

355 4.2.2 EFFICIENCY ANALYSIS

356 Table 3 reports the efficiency of MemArt against baselines on LoCoMo. Prefill efficiency is measured by the
 357 number of tokens computed per request, while decode efficiency is measured by the effective KV length.

358 For prefill, MemArt requires only 32 and 37 tokens on average for each request with LLaMA and Qwen,
 359 respectively, since it computes only the new query while reusing retrieved KV blocks. In contrast, plaintext-
 360 based methods (Zep, Mem0) must recompute all retrieved tokens, leading to 91–135× more prefill tokens.
 361 **H2O, which computes the entire KV cache during prefill and defers pruning to decode, therefore incurs a**
 362 **similarly high prefill cost.** Compared with FullContext inference and H2O, MemArt achieves an additional
 363 598–684× reduction. For decoding, MemArt processes only the KV blocks selected for retrieval plus the
 364 current KV cache of query, reducing KV length by 0.6%–36.4% over Zep, Mem0 and H2O and by 81.2%–
 365 90.4% over FullContext.

366 End-to-end latency results in Figure 4 confirm these gains: despite KV selection and I/O overhead, MemArt
 367 delivers up to 2.30× and 2.38× speedup over Zep and Mem0, 13.70× over H2O and 9.9–15.8× speedup
 368 over FullContext.

370 4.2.3 ABLATION STUDY

372 Figure 5 evaluates different multi-token aggregation retrieval strategies in MemArt on LLaMA3.1-8B-
 373 Instruct and Qwen2.5-7B-Instruct. Each memory block is scored by normalizing per-token relevance
 374 $I(Q, K)$ (Table 1) and aggregating across query tokens. We compare Softmax vs. Reciprocal Rank (RR)
 375 normalization, Sum vs. Max aggregation, and varying block sizes. Results show that Max aggregation con-

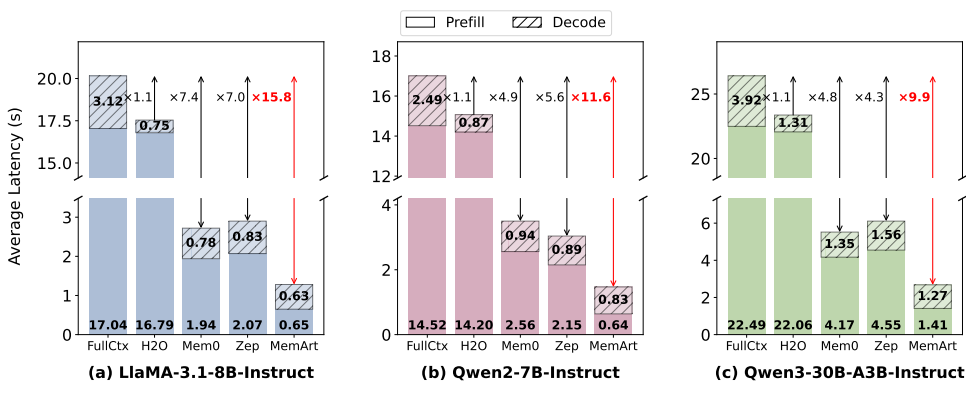


Figure 4: The average request execution latency of different methods.

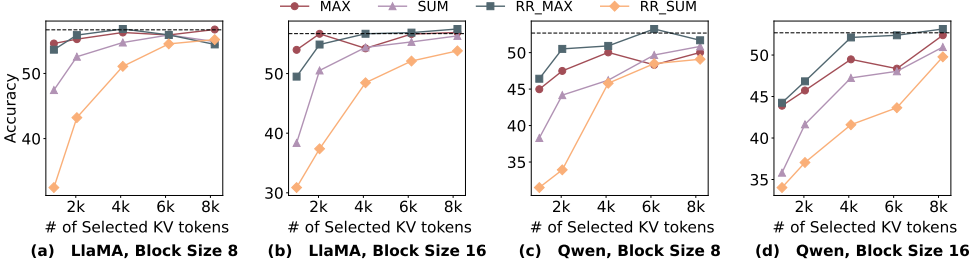


Figure 5: Ablation study of multi-token aggregation retrieval strategies.

sistently outperforms Sum, especially with fewer retrieved tokens, highlighting the benefit of emphasizing the strongest query-block interaction. Between normalization methods, Softmax and RR perform similarly on LLaMA, while RR-Max is superior on Qwen. Retrieval accuracy is largely insensitive to block size (8 vs. 16). In general, the choice of aggregation dominates the retrieval quality, while normalization and block size play secondary roles.

Table 4: Latency breakdown when storing KVCache in HBM vs. DRAM (Llama-3.1-8B-Instruct, 14k context).

Method /Time(ms)	Attn	FFN	re-RoPE	Sel. TopK	Mem. Ops
Full Ctx	10,072.7	5,397.2	0.0	0.0	0.0
MemArt (HBM)	17.9	23.5	5.5	117.5	29.9
MemArt (DRAM)	18.1	22.9	5.4	111.7	237.8

Table 4 details the latency breakdown of the prefilling phase when storing the 14k-token KV cache in HBM versus DRAM for the Llama-3.1-8B-Instruct model. The dramatic reduction in Attn and FFN latency is attributed to the significantly reduced computational scope: in contrast to the full context baseline ($14k \times 14k$), MemArt computes attention using a query length of 32 against a retrieved context of $32 + 2048$. This results in an over $2900\times$ reduction in FLOPs.

Similarly, the FFN operates on a sequence length of only 32, compared to 14k in the baseline. The positional re-encoding adds a trivial 5.5 ms latency, while the cost of Top-K selection is acceptable due to our compressed key representation (AABB). Consequently, the primary latency bottleneck shifts to cross-tier memory transfers, specifically the migration of KV blocks from DRAM to HBM via PCIe. Note that these results reflect a naive, fully serialized implementation; this overhead can be substantially mitigated in future iterations through prefetching and overlapped compute.

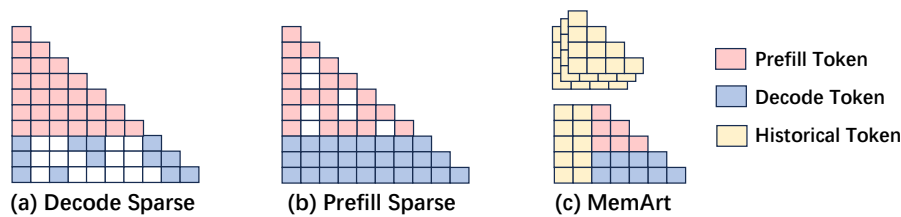


Figure 6: Comparison of attention mechanisms between MemArt and sparse attention.

5 DISCUSSIONS

Differences from Sparse Attention Methods Although MemArt and sparse attention methods share the principle of utilizing the attention mechanism to identify salient information, they are fundamentally distinct. The primary differences lie in their temporal scope, core purpose, and the source of their attention scores. Specifically, sparse attention focuses on in-session acceleration by employing self-attention over the current context for sparsity, while MemArt targets memory-augmented generation by leveraging Query-Memory cross-attention over current and historical context for retrieval.

As shown in Figure 6, sparse attention generally falls into two categories. Decode sparse methods (e.g., H2O (Zhang et al., 2023), Infill (Xiao et al., 2024), Quest (Tang et al., 2024) and ArkVale (Chen et al., 2024)) maintain full attention during prefill but selectively compute important tokens at each decoding step. Prefill sparse methods (e.g., MInference (Jiang et al., 2024) and NSA (Yuan et al., 2025)) introduce sparsity by restricting each query token during the prefill stage to attend only to a subset of keys. The core goal of both categories is to accelerate the current inference speed or reduce the in-session KV Cache memory footprint, rather than to enhance long-horizon generation quality. Their sparsity is determined by self-attention over the current context window to infer which content is unimportant or redundant, thereby reducing computation.

In contrast, MemArt is an external, persistent long-term memory system whose primary goal is to significantly enhance the model’s reasoning and generation quality. MemArt operates across a temporal divide: it performs retrieval once, prior to the prefill stage, injecting historical KV blocks from past sessions directly into the computation. Its attention scores are derived from cross-session cross-attention between the current request (Query) and the historical memory blocks (Keys), judging which historical information is most relevant and enhancing for the current inference. This essential spatio-temporal leap (historical data vs. current inference) and the blending of external retrieval with internal computation fundamentally distinguish MemArt from all sparse attention methods, providing the unique capability of long-horizon, non-contiguous memory recall.

6 CONCLUSION

This paper introduced MemArt, a paradigm that shifts agent memory from plaintext to the LLM’s native KV cache. Our experiments on the LoCoMo benchmark show that this KVCache-centric approach is not only dramatically more efficient—reducing prefill tokens by over $90\times$ —but also more accurate, improving accuracy by over 11%. Our work demonstrates that operating in the model’s latent state is a more powerful and promising foundation for agent memory. Future research could explore learned KV cache compression and more sophisticated retrieval strategies. The code for MemArt will be made publicly available to encourage further exploration in this direction.

470 REPRODUCIBILITY STATEMENT
471472 We provide the necessary code, datasets, evaluation scripts, and the raw data used to derive our experimental
473 conclusions in the supplementary material to ensure reproducibility.
474475 REFERENCES
476477 Amazon Web Services. Add memory to your ai agent – amazon bedrock agentcore docu-
478 mentation. <https://docs.aws.amazon.com/bedrock-agentcore/latest/devguide/memory.html>, 2025.
479480 Panpan Cai, Chandrasekaran Indhumathi, Yiyu Cai, Jianmin Zheng, Yi Gong, Teng Sam Lim, and Peng
481 Wong. Collision detection using axis aligned bounding boxes. In *Simulations, Serious Games and Their*
482 *Applications*, pp. 1–14, 2014.
483484 Renze Chen, Zhuofeng Wang, Beiquan Cao, Tong Wu, Size Zheng, Xiuhong Li, Xuechao Wei, Shengen Yan,
485 Meng Li, and Yun Liang. Arkvale: Efficient generative llm inference with recallable key-value eviction.
486 In *Proceedings of the Thirty-eighth Annual Conference on Neural Information Processing Systems*, pp.
487 113134–113155, 2024.
488489 Prateek Chhikara, Dev Khant, Saket Aryan, Taranjeet Singh, and Deshraj Yadav. Mem0: Building
490 production-ready ai agents with scalable long-term memory. *arXiv preprint arXiv:2504.19413*, 2025.
491492 Gordon V Cormack, Charles L A Clarke, and Stefan Büttcher. Reciprocal rank fusion outperforms condorcet
493 and individual rank learning methods. In *Proceedings of the 32nd international ACM SIGIR conference*
494 *on Research and development in information retrieval*, pp. 758–759, 2009.
495496 Alessio Devoto, Yu Zhao, Simone Scardapane, and Pasquale Minervini. A simple and effective L_2 norm-
497 based strategy for KV cache compression. 2024.
498499 Bin Gao, Zhuomin He, Puru Sharma, Qingxuan Kang, Djordje Jevdjic, Junbo Deng, Xingkun Yang, Zhou
500 Yu, and Pengfei Zuo. Cost-efficient large language model serving for multi-turn conversations with cache-
501 dattention. In *Proceedings of the 2024 USENIX Annual Technical Conference*, pp. 111–126, 2024.
502503 Google DeepMind. Gemini 2.5 pro. <https://blog.google/technology/google-deepmind/gemini-model-thinking-updates-march-2025/>, 2025.
504505 Aaron Grattafiori, Abhimanyu Dubey, Abhinav Jauhri, Abhinav Pandey, Abhishek Kadian, Ahmad Al-
506 Dahle, Aiesha Letman, Akhil Mathur, Alan Schelten, Alex Vaughan, Amy Yang, Angela Fan, Anirudh
507 Goyal, Anthony Hartshorn, Aobo Yang, Archi Mitra, Archie Sravankumar, Artem Korenev, Arthur
508 Hinsvark, Arun Rao, Aston Zhang, Aurelien Rodriguez, Austen Gregerson, Ava Spataru, Baptiste
509 Roziere, Bethany Biron, Binh Tang, Bobbie Chern, Charlotte Caucheteux, Chaya Nayak, Chloe Bi, Chris
510 Marra, Chris McConnell, and et al. The llama 3 herd of models. *arXiv preprint arXiv:2407.21783*, 2024.
511512 Harold Hotelling. Analysis of a complex of statistical variables into principal components. *Journal of*
513 *Educational Psychology*, 24(6):417–441, 1933.
514515 Bowen Jiang, Zhuoqun Hao, Young-Min Cho, Bryan Li, Yuan Yuan, Sihao Chen, Lyle Ungar, Camillo J
516 Taylor, and Dan Roth. Know me, respond to me: Benchmarking llms for dynamic user profiling and
personalized responses at scale. *arXiv preprint arXiv:2504.14225*, 2025.
517

517 Huiqiang Jiang, Yucheng Li, Chengruidong Zhang, Qianhui Wu, Xufang Luo, Surin Ahn, Zhenhua Han,
 518 Amir H. Abdi, Dongsheng Li, Chin-Yew Lin, Yuqing Yang, and Lili Qiu. MInference 1.0: Accelerating
 519 pre-filling for long-context LLMs via dynamic sparse attention. In *Proceedings of the Thirty-eighth*
 520 *Annual Conference on Neural Information Processing Systems*, pp. 52481–52515, 2024.

521

522 Jiazheng Kang, Mingming Ji, Zhe Zhao, and Ting Bai. Memory os of ai agent. *arXiv preprint*
 523 *arXiv:2506.06326*, 2025.

524

525 Woosuk Kwon, Zhuyun Liu, Haiyang Zheng, Xi Li, Ying Zhang, Ziyan Fu, Yuhong Han, Xing Huang, and
 526 Zhaonan Zhao. Efficient memory management for large language model serving with pagedattention. In
 527 *Proceedings of the 29th ACM Symposium on Operating Systems Principles*, pp. 611–626, 2023.

528

529 Zhiyu Li, Shichao Song, Chenyang Xi, Hanyu Wang, Chen Tang, Simin Niu, Ding Chen, Jiawei Yang,
 530 Chunyu Li, Qingchen Yu, Jihao Zhao, Yezhaohui Wang, Peng Liu, Zehao Lin, Pengyuan Wang, Jiahao
 531 Huo, Tianyi Chen, Kai Chen, Kehang Li, Zhen Tao, Huayi Lai, Hao Wu, Bo Tang, Zhenren Wang,
 532 Zhaoxin Fan, Ningyu Zhang, Linfeng Zhang, Junchi Yan, Mingchuan Yang, Tong Xu, Wei Xu, Huajun
 533 Chen, Haofen Wang, Hongkang Yang, Wentao Zhang, Zhi-Qin John Xu, Siheng Chen, and Feiyu Xiong.
 534 Memos: A memory os for AI system. *arXiv preprint arXiv:2507.03724*, 2025.

535

536 Junwei Liu, Kaixin Wang, Yixuan Chen, Xin Peng, Zhenpeng Chen, Lingming Zhang, and Yiling Lou. Large
 537 language model-based agents for software engineering: A survey. *arXiv preprint arXiv:2409.02977*, 2024.

538

539 Adyasha Maharana, Dong-Ho Lee, Sergey Tulyakov, Mohit Bansal, Francesco Barbieri, and Yuwei Fang.
 540 Evaluating very long-term conversational memory of llm agents. *arXiv preprint arXiv:2402.17753*, 2024.

541

542 Charles Packer, Vivian Fang, Shishir G Patil, Kevin Lin, Sarah Wooders, and Joseph E Gonzalez. Memgpt:
 543 Towards llms as operating systems. *arXiv preprint arXiv:2310.08560*, 2023.

544

545 Ruoyu Qin, Zheming Li, Weiran He, Jialei Cui, Feng Ren, Mingxing Zhang, Yongwei Wu, Weimin Zheng,
 546 and Xinran Xu. Mooncake: Trading more storage for less computation—a kvcache-centric architecture
 547 for serving llm chatbot. In *Proceedings of the 23rd USENIX Conference on File and Storage Technologies*,
 548 pp. 155–170, 2025.

549

550 Preston Rasmussen, Pavlo Paliychuk, Travis Beauvais, Jack Ryan, and Daniel Chalef. Zep: A temporal
 551 knowledge graph architecture for agent memory. *arXiv preprint arXiv:2501.13956*, 2025.

552

553 Jianlin Su, Murtadha Ahmed, Yu Lu, Shengfeng Pan, Wen Bo, and Yunfeng Liu. Roformer: Enhanced
 554 transformer with rotary position embedding. *Neurocomputing*, 568(C), 2024.

555

556 Jiaming Tang, Yilong Zhao, Kan Zhu, Guangxuan Xiao, Baris Kasikci, and Song Han. Quest: query-aware
 557 sparsity for efficient long-context llm inference. In *Proceedings of the 41st International Conference on*
 558 *Machine Learning*, pp. 47901–47911, 2024.

559

560 Gino Van den Bergen. Efficient collision detection of complex deformable models using AABB trees.
 561 *Journal of Graphics Tools*, 2(4):1–13, 1997.

562

563 Lei Wang, Chen Ma, Xueyang Feng, Zeyu Zhang, Hao Yang, Jingsen Zhang, Zhiyuan Chen, Jiakai Tang,
 564 Xu Chen, Yankai Lin, Wayne Xin Zhao, Zhewei Wei, and Jirong Wen. A survey on large language model
 565 based autonomous agents. *Frontiers of Computer Science*, 18(6), 2024a.

566

567 Zheng Wang, Boxiao Jin, Zhongzhi Yu, and Minjia Zhang. Model tells you where to merge: Adaptive kv
 568 cache merging for llms on long-context tasks. *arXiv preprint arXiv:2407.08454*, 2024b.

564 Thomas Wolf, Lysandre Debut, Victor Sanh, Julien Chaumond, Clement Delangue, Anthony Moi, Pier-
 565 ric Cistac, Tim Rault, Rémi Louf, Morgan Funtowicz, Joe Davison, Sam Shleifer, Patrick von Platen,
 566 Clara Ma, Yacine Jernite, Julien Plu, Canwen Xu, Teven Le Scao, Sylvain Gugger, Mariama Drame,
 567 Quentin Lhoest, and Alexander M. Rush. Transformers: State-of-the-art natural language processing.
 568 In *Proceedings of the 2020 Conference on Empirical Methods in Natural Language Processing: System
 569 Demonstrations*, pp. 38–45, 2020.

570 Chaojun Xiao, Pingle Zhang, Xu Han, Guangxuan Xiao, Yankai Lin, Zhengyan Zhang, Zhiyuan Liu, and
 571 Maosong Sun. InfLLM: Training-free long-context extrapolation for LLMs with an efficient context mem-
 572 ory. In *Proceedings of the Thirty-eighth Annual Conference on Neural Information Processing Systems*,
 573 pp. 119638–119661, 2024.

574 Renjun Xu and Jingwen Peng. A comprehensive survey of deep research: Systems, methodologies, and
 575 applications. *arXiv preprint arXiv:2506.12594*, 2025.

577 Wujiang Xu, Kai Mei, Hang Gao, Juntao Tan, Zujie Liang, and Yongfeng Zhang. A-mem: Agentic memory
 578 for llm agents. *arXiv preprint arXiv:2502.12110*, 2025.

580 Sikuan Yan, Xiufeng Yang, Zuchao Huang, Ercong Nie, Zifeng Ding, Zonggen Li, Xiaowen Ma, Hinrich
 581 Schütze, Volker Tresp, and Yunpu Ma. Memory-r1: Enhancing large language model agents to manage
 582 and utilize memories via reinforcement learning. *arXiv preprint arXiv:2508.19828*, 2025.

583 An Yang, Anfeng Li, Baosong Yang, Beichen Zhang, Binyuan Hui, Bo Zheng, Bowen Yu, Chang Gao,
 584 Chengen Huang, Chenxu Lv, Chujie Zheng, Dayiheng Liu, Fan Zhou, Fei Huang, Feng Hu, Hao Ge,
 585 Haoran Wei, Huan Lin, Jialong Tang, Jian Yang, Jianhong Tu, Jianwei Zhang, Jianxin Yang, Jiaxi Yang,
 586 Jing Zhou, Jingren Zhou, Junyang Lin, Kai Dang, Keqin Bao, Kexin Yang, Le Yu, Lianghao Deng, Mei Li,
 587 Mingfeng Xue, Mingze Li, Pei Zhang, Peng Wang, Qin Zhu, Rui Men, Ruize Gao, Shixuan Liu, Shuang
 588 Luo, Tianhao Li, Tianyi Tang, Wenbiao Yin, Xingzhang Ren, Xinyu Wang, Xinyu Zhang, Xuancheng
 589 Ren, Yang Fan, Yang Su, Yichang Zhang, Yinger Zhang, Yu Wan, Yuqiong Liu, Zekun Wang, Zeyu Cui,
 590 Zhenru Zhang, Zhipeng Zhou, and Zihan Qiu. Qwen3 technical report. *arXiv preprint arXiv:2505.09388*,
 591 2025a.

592 An Yang, Baosong Yang, Beichen Zhang, Binyuan Hui, Bo Zheng, Bowen Yu, Chengyuan Li, Dayiheng
 593 Liu, Fei Huang, Haoran Wei, Huan Lin, Jian Yang, Jianhong Tu, Jianwei Zhang, Jianxin Yang, Jiaxi Yang,
 594 Jingren Zhou, Junyang Lin, Kai Dang, Keming Lu, Keqin Bao, Kexin Yang, Le Yu, Mei Li, Mingfeng
 595 Xue, Pei Zhang, Qin Zhu, Rui Men, Runji Lin, Tianhao Li, Tianyi Tang, Tingyu Xia, Xingzhang Ren,
 596 Xuancheng Ren, Yang Fan, Yang Su, Yichang Zhang, Yu Wan, Yuqiong Liu, Zeyu Cui, Zhenru Zhang,
 597 and Zihan Qiu. Qwen2.5 technical report. *arXiv preprint arXiv:2412.15115*, 2025b.

598 Jiayi Yao, Hanchen Li, Yuhan Liu, Siddhant Ray, Yihua Cheng, Qizheng Zhang, Kuntai Du, Shan Lu, and
 599 Zexi Jiang. Cacheblend: Fast large language model serving for rag with cached knowledge fusion. In
 600 *Proceedings of the 20th European Conference on Computer Systems*, pp. 94–109, 2025.

602 Jingyang Yuan, Huazuo Gao, Damai Dai, Junyu Luo, Liang Zhao, Zhengyan Zhang, Zhenda Xie, Yuxing
 603 Wei, Lean Wang, Zhiping Xiao, Yuqing Wang, Chong Ruan, Ming Zhang, Wenfeng Liang, and Wangding
 604 Zeng. Native sparse attention: Hardware-aligned and natively trainable sparse attention. In *Proceedings
 605 of the 63rd Annual Meeting of the Association for Computational Linguistics*, pp. 23078–23097, 2025.

606 Zhenyu Zhang, Ying Sheng, Tianyi Zhou, Tianlong Chen, Lianmin Zheng, Ruisi Cai, Zhao Song, Yuandong
 607 Tian, Christopher Re, Clark Barrett, Zhangyang Wang, and Beidi Chen. H2o: Heavy-hitter oracle for effi-
 608 cient generative inference of large language models. In *Thirty-seventh Conference on Neural Information
 609 Processing Systems*, 2023.

611 Lianmin Zheng, Liangsheng Yin, Zhiqiang Xie, Chuyue Livia Sun, Jeff Huang, Cody Hao Yu, Shiyi Cao,
 612 Christos Kozyrakis, Ion Stoica, Joseph E Gonzalez, et al. Sqlang: Efficient execution of structured lan-
 613 guage model programs. *Proceedings of the Thirty-eighth Annual Conference on Neural Information Pro-*
 614 *cessing Systems*, pp. 62557–62583, 2024.

615 Wanjun Zhong, Lianghong Guo, Qiqi Gao, He Ye, and Yanlin Wang. Memorybank: enhancing large lan-
 616 guage models with long-term memory. In *Proceedings of the Thirty-Eighth AAAI Conference on Artificial*
 617 *Intelligence*, 2024.

619 A APPENDIX

620 A.1 STATEMENT ON THE USE OF LLMs

621 We used a large language model (ChatGPT) solely as a writing assistant to polish the language of this paper,
 622 such as improving grammar and clarity. The model was not involved in research ideation, methodological
 623 design, data analysis, or interpretation of results. All scientific content and conclusions were conceived and
 624 verified entirely by the authors.

625 A.2 STRATEGY ABLATION ACROSS MULTIPLE METRICS

626 Figure 7 provides a granular view of the retrieval strategy ablation study, broken down by evaluation metric.
 627 The results reinforce the main findings presented in the body of the paper. We observe several consistent
 628 trends across all model and block-size configurations:

- 629 • Max aggregation is consistently superior to Sum, especially when retrieving a smaller number of
 630 tokens.
- 631 • On LLaMA, Softmax and Reciprocal-Rank (RR) normalization perform comparably, while the
 632 RR-Max combination yields the best results on Qwen.
- 633 • Retrieval accuracy shows low sensitivity to block size (8 vs. 16), suggesting the approach is robust.

634 Overall, the aggregation method is the dominant factor in retrieval quality, with normalization and block size
 635 playing secondary roles.

636 A.3 THE IMPORTANCE OF DECOUPLED POSITIONAL ENCODING

637 The necessity of decoupling positional encodings for reliable long-term memory is illustrated in the case
 638 study shown in Figure 8. In this experiment, we load the system with a large historical context (approx. 1M
 639 tokens) and compare performance with and without our decoupling mechanism.

640 As shown, when reusing KV cache with the standard, coupled positional encoding, the model’s positional
 641 awareness breaks down once the context length exceeds its native window size. This misalignment leads to a
 642 catastrophic failure, resulting in degenerative, repetitive text. In contrast, our decoupled positional encoding
 643 mechanism completely resolves this issue, enabling the model to correctly utilize information from the
 644 distant past and generate a coherent answer. This demonstrates that decoupling is not just an optimization
 645 but an essential component for enabling robust, long-term memory in KVCache-centric systems.

646 A.4 INTERPRETABILITY CASE STUDIES

647 In this section, we provide the case study to illustrate how MemArt retrieves and uses historical KV blocks.
 648 This case consists of: (1) A KV-to-text-span mapping, showing the original textual segment corresponding

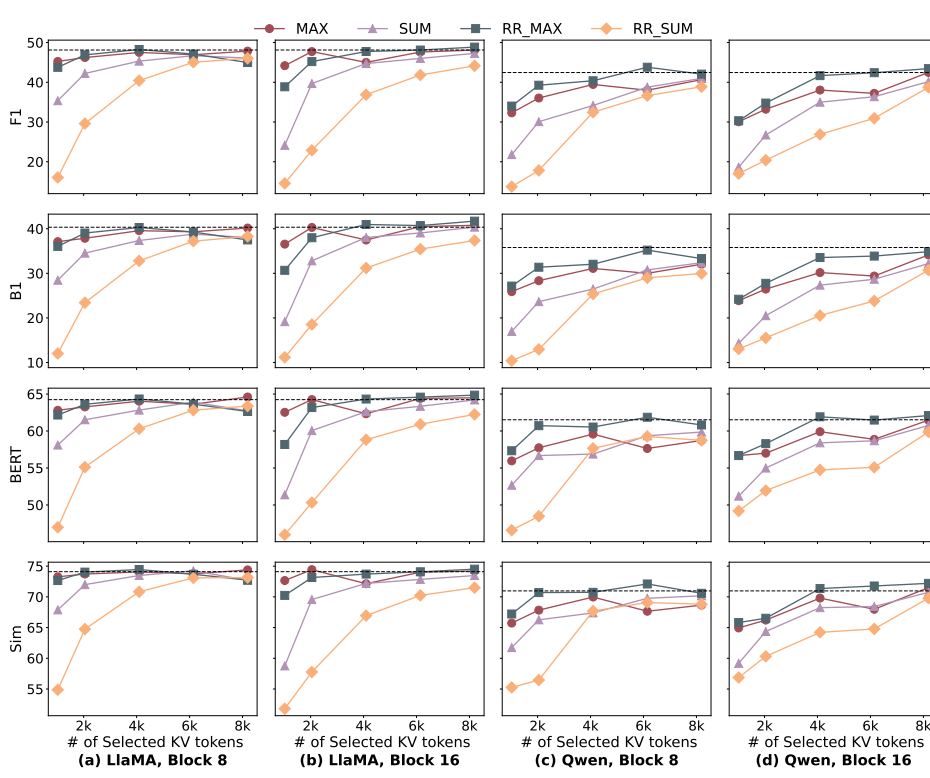


Figure 7: Ablation study of retrieval strategies on LLaMA and Qwen models with block sizes 8 and 16, evaluated across F1, B1, BERT, and Sim metrics.

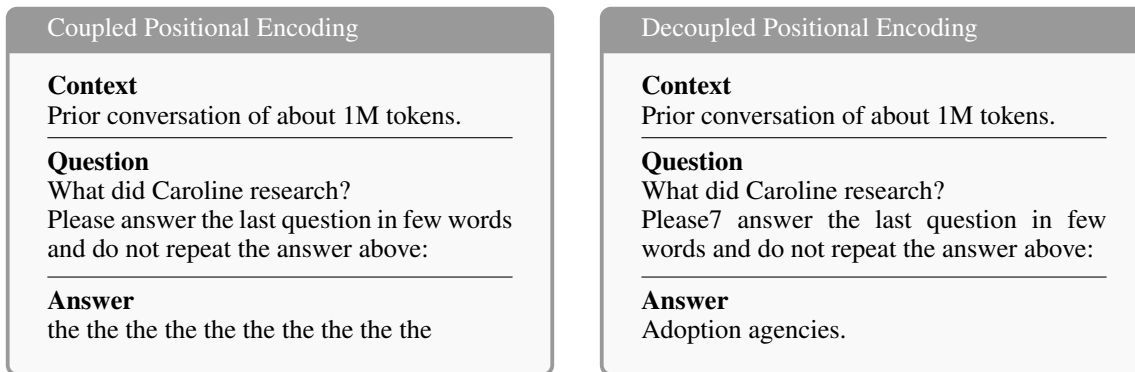


Figure 8: Case study on the importance of positional encoding decoupling for long-term memory.

to the retrieved KV block and (2) A layer-wise rank trajectory plot, showing how the relevance rank of this segment evolves across transformer layers.

705
706
707
708
709
710
711
712
713

Retrieved Text Span

Query and Gold Answer

Q: What did Caroline research?
A: Adoption agencies.

Crucial Context Excerpt

Caroline: Researching adoption agencies
— it's been ...

(a) KV-to-text-span mapping for the retrieved block.

Layer Index	Number of Layers
3	45
4	60
5	55
6	65
7	70
8	85
9	10
10	20
11	25
12	30
13	35
14	40
15	25
16	30
17	35
18	30
19	25
20	20
21	25
22	30
23	25
24	20
25	25
26	75
27	60
28	55
29	50
30	40

(b) Layer-wise rank trajectory of the retrieved block.

Figure 9: Interpretability case study for the query “*What did Caroline research?*”. (a) textual span corresponding to a retrieved KV block. (b) layer-wise rank trajectory of the block.

Figure 9 presents a qualitative analysis designed to improve interpretability of MemArt’s retrieval behavior. For the example query “What did Caroline research?”, the retrieved block contains the phrase “Caroline: Researching adoption agencies — ...” shown in the left panel. The right panel plots the layer-wise rank trajectory of this KV block across the Llama’s 32 transformer layers. The block begins with moderate relevance (e.g., ranks 35, 64, 51 of 920) but rapidly rises into the top ranks after Layer 10 and remains consistently within the top-5 most relevant blocks in deeper layers.

Together, the text-span visualization and rank trajectory show not only which block MemArt retrieves, but also how strongly and consistently the model relies on it across layers. This combined evidence demonstrates that MemArt retrieves semantically correct and persistent information rather than relying on incidental correlations.

730

A.5 ROBUSTNESS OF MEMART UNDER ADVERSARIAL QUERIES

733

To evaluate the robustness of MemArt under adversarial, we conducted an additional experiment on the LoCoMo adversarial request subset using a strict factuality probing prompt: *“If the answer is not explicitly stated or directly inferable, respond only with: ‘I don’t know’.”*

736
737
738
739

This setup tests whether the MemArt retrieval essential blocks required to avoid hallucination. On 100 adversarial queries, the full-context baseline produced 61 correct “I don’t know” responses, while MemArt produced 57. The near-identical behavior indicates that our design preserves the relevant blocks even under adversarial queries and maintains generation correctness.

740

741

A.6 MULTI-AGENT MEMORY COMPATIBILITY

743

MemArt can cleanly integrate into multi-agent environments, even when agents run heterogeneous models. The key idea is to preserve a model-agnostic communication channel across agents, while allowing each agent to maintain its own model-specific internal memory.

746

747

Inter-agent sharing: When heterogeneous agents need to communicate, they can exchange information through plaintext such as raw text, summaries, or structured memory, which remains model-agnostic.

748
749
750
751

Intra-agent memory: Once an agent consumes this information even once, it is encoded into its own KV cache and stored as MemArt blocks. Any future reuse of that information is purely an internal process. Subsequent retrieval relies solely on the agent's own representational space, enabling high-fidelity recall and compute efficiency without affecting cross-agent communication.

752 Thus, MemArt naturally coexists with multi-agent: plaintext memory remains the system-level lingua franca,
 753 while MemArt functions as a private, high-performance retrieval layer for each agent. This makes MemArt
 754 fully compatible with heterogeneous multi-agent systems: agents communicate externally in text, but inter-
 755 nationally obtain the benefits of KV-native long-term memory.
 756

757 A.7 ADDITIONAL EVALUATION ON PERSONAMEM

759 PersonaMem (Jiang et al., 2025) is a challenging long-horizon, multi-session dialogue benchmark specif-
 760 ically designed to assess an agent’s ability to recall personalized, non-contiguous, and session-spanning
 761 information. Each instance features multi-turn conversations across several sessions, totaling an average
 762 context length of approximately 32K tokens. The task is evaluated using accuracy (correct answer rate)
 763 based on multiple-choice questions provided per instance.

764 Table 5: Accuracy comparison between MemArt and baselines on the PersonaMem benchmark. Best scores
 765 are in bold and second-best are underlined.
 766

767 Model	768 FullContext	769 Zep	770 Mem0	771 H2O	772 MemArt
769 L3	46.52	40.57	38.37	37.18	<u>44.82</u>
770 Q2	54.50	47.20	47.37	48.73	<u>52.97</u>
771 Q3	59.93	50.59	53.48	51.27	<u>58.91</u>

772 We evaluate MemArt against FullContext, Zep, Mem0, and H2O across Llama3.1-8B-Instruct(L3),
 773 Qwen2.5-7B-Instruct(Q2) and Qwen3-30B-A3B-Instruct(Q3) using the standard accuracy metric. Across all
 774 models, MemArt provides consistent and substantial gains over plaintext memory systems and KV-pruning
 775 baselines. Relative to Zep and Mem0, MemArt improves accuracy by 10.4%/16.8% on L3, 12.2%/11.8% on
 776 Q2, and 16.4%/10.1% on Q3, respectively. Compare to H2O, MemArt improves accuracy by 20.5% on L3,
 777 8.7% on Q2, and 14.9% on Q3, respectively. Overall, these gains confirm that MemArt generalizes beyond
 778 LoCoMo and provides robust long-horizon recall for multi-session agent trace.
 779

780 A.8 SYSTEM-LEVEL CONSIDERATIONS: MEMORY I/O AND STORAGE

782 MemArt introduces a memory pool of historical KV blocks, which raises two system-level considerations:
 783 access latency and long-term storage growth. These concerns are inherent to all KV-centric serving archi-
 784 tectures—not unique to our approach—as modern systems such as vLLM, SGLang, and Mooncake already
 785 persist and retrieve KV caches to enable prefix caching and reduce recomputation. MemArt follows the same
 786 principle but generalizes it to non-contiguous historical segments for long-horizon recall. Memory-pool I/O
 787 (HBM–DRAM transfers, prefetching, overlap with compute) is largely orthogonal to our algorithmic contribu-
 788 tions; standard system optimizations such as asynchronous I/O, hierarchical caching, and double-buffering
 789 can be directly adopted. Similarly, MemArt is fully compatible with existing KV cache compression tech-
 790 niques (Devoto et al., 2024; Wang et al., 2024b), which can be layered on top to reduce storage footprint and
 791 further mitigate memory growth.
 792